Mon. Not. R. Astron. Soc. **000**, 000–000 (2001)

On the lack of cold dust in IRAS P09104+4109 and IRAS F15307+3252 – their spectral energy distributions and implications for finding dusty AGNs at high redshift

J. R. Deane[1] and Neil Trentham[2]
[1] *Physics Department, Queen Mary and Westfield College, Mile End Road, London E1 4NS*
[2] *Institute of Astronomy, Madingley Road, Cambridge, CB3 0HA.*

29 May 2001

ABSTRACT

We present upper limits on the 850 μm and 450 μm fluxes of the warm hyperluminous (bolometric luminosity $L_{\rm bol} > 10^{13}\,{\rm L}_{\odot}$) galaxies IRAS P09104+4109 ($z = 0.442$) and IRAS F15307+3252 ($z = 0.926$), derived from measurements using the SCUBA bolometer array on the James Clerk Maxwell Telescope. Hot luminous infrared sources like these are thought to differ from more normal cold ultraluminous infrared ($L_{\rm bol} > 10^{12}\,{\rm L}_{\odot}$) galaxies in that they derive most of their bolometric luminosities from dusty AGNs as opposed to starbursts. Such hot, dusty AGNs at high redshift are thought to be responsible for much of the mass accretion of the Universe that is in turn responsible for the formation of the supermassive black holes seen in the centres of local galaxies. The galaxy IRAS P09104+4109 is also unusual in that it is a cD galaxy in the center of a substantial cooling-flow cluster, not an isolated interacting galaxy like most ultraluminous infrared galaxies. Previously it was known to have large amounts of hot ($T > 50$ K) dust from *IRAS* observations. We now show that the contribution of cold dust to the bolometric luminosity is less than 3 per cent. Most ultraluminous infrared galaxies possess large amounts of cold dust, and it is now known that some cooling flow cluster cD galaxies do as well. Yet this object, which is an extreme example of both, does not have enough cold gas to contribute significantly to the bolometric luminosity. We outline physical reasons why this could have happened. We then provide a discussion of stategies for finding hot dusty AGNs, given the limitations on submillimetre surveys implied by this work.

Key words: infrared: galaxies – quasars: general – cosmology: observations – galaxies: individual: IRAS P09104+4109 – galaxies: individual: IRAS F15307+3252

1 INTRODUCTION

Two extreme ultraluminous infrared galaxies (ULIGs) at redshifts $z < 1$ that are thought to derive most of their bolometric luminosity from a dust-enshrouded active galactic nuclei (AGNs) are IRAS P09104+4109 and IRAS F15307+3252. These objects differ from optical quasars, even those with "infrared bumps" (e.g. Sanders et al. 1989), in that they are very faint at rest-frame optical wavelengths; their B-band luminosities are at least an order of magnitude lower than their 25-μm luminosities, for example. These kinds of objects have attracted much recent attention because of the possibility that much of the mass accretion in the Universe responsible for producing the high local density of supermassive black holes (Magorrian et al. 1998) might have occurred in high redshift analogues of these two galaxies (Haehnelt, Natarajan & Rees 1998; Fabian & Iwasawa 1999; Salucci et al. 1999).

The galaxy IRAS P09104+4109 was identified by Kleinmann et al. (1988) to be an ultraluminous IRAS galaxy at $z = 0.442$. It was found in a follow-up survey of *IRAS* 60-μm sources that had non-stellar colours and no optical counterparts on the Palomar Sky Survey. Its bolometric luminosity is $1.4 \times 10^{13}\,{\rm L}_{\odot}$, which is extremely high, even for a ULIG (it would be classed as a hyperluminous infrared galaxy by Sanders & Mirabel 1996). Radio, optical, near- and mid-infrared imaging, spectroscopy, and spectropolarimetry (Kleinmann et al. 1988, Hines & Wills 1993, Soifer et al. 1996, Green & Rowan-Robinson 1996; Taniguchi et al. 1997, Evans et al. 1998, Hines et al 1999) suggest that this galaxy is powered by an obscured AGN. A hard X-ray detection of IRAS P09104+4109 with *BeppoSax* (Frances-

chini et al. 2000) confirms that this object contains a powerful AGN.

The spectral energy distribution (SED) of IRAS P09104+4109 is unusual in that it peaks between 10 and 30 μm, implying that the dust responsible for reradiating the energy from the obscured AGN must be very hot, in excess of 100 K. This is very different from what is seen in other powerful (although lower in luminosity than IRAS P09104+4109) dust-enshrouded AGNs like the "warm" ULIGs Markarian 231 and IRAS 08572+3915 (Sanders et al. 1988a). These have dust temperatures closer to 50 K and SEDs which peak longward of 50 μm. The dust in IRAS P09104+4109 is also considerably hotter than the dust in many infrared QSOs, like Markarian 1014 (Sanders et al. 1988b). That the dust in IRAS P09104+4109 is so much hotter than the dust in other ULIGs hosting powerful AGNs is perhaps suggestive that the dust in IRAS P09104+4109 is being heated directly by the AGN whereas in the other ULIGs, much of the far-infrared luminosity comes from colder, more diffuse, dust heated by star formation (Rowan-Robinson & Crawford 1989, Rowan-Robinson & Efstathiou 1993, Rowan-Robinson 2000).

Additionally, IRAS P09104+4109 is a cD galaxy in a rich X-ray cluster that is undergoing a very substantial cooling flow, about 1000 $M_\odot$ yr^{-1} (Fabian & Crawford 1995, Crawford & Vanderriest 1996). In this way it is very different from other ULIGs, which are normally isolated peculiar galaxies, often showing signs of a recent interaction (Sanders et al. 1988a, Clements et al. 1996, Murphy et al. 1996).

So IRAS P09104+4109 is a very unusual ULIG on three grounds: (i) its bolometric luminosity is very high; (ii) its SED is peaked at short wavelengths, implying a much higher dust temperature; and (iii) it is not a peculiar galaxy, but a cD galaxy in the center of a massive X-ray cluster that is undergoing a cooling flow.

It is interesting to speculate as to whether these properties are related; in particular one might ask whether or not the cooling flow can fuel the AGN and in doing so generate the high bolometric luminosity and dust temperature. A related question is: does IRAS P09104+4109 have any cold ($T \leq 50$ K) dust at all, or is all the dust in this galaxy extremely hot and directly associated with the AGN. Almost all other ULIGs (Sanders & Mirabel 1996) and some high-redshift quasars (McMahon et al. 1999) possess cold gas. Some cooling flow clusters do too, as inferred from their SCUBA submillimetre detections (Edge et al. 1999) and CO line measurements (e.g. Bridges & Irwin 1998). Cooling flow clusters also tend to have star-formation in progress at their centers (Cardiel et al. 1998, Crawford et al. 1999), which may be fuelled by this cold gas. This star formation could could directly produce the dust seen by Edge and collaborators. In IRAS P09104+4109, we have the additional evidence that there exists a high column density of X-ray absorbing gas (Iwasawa, Fabian & Ettori 2001) which is likely to be cold.

The galaxy IRAS F15307+3252 ($z = 0.926$; Cutri et al. 1994) is another hyperluminous infrared galaxy thought to be powered by a luminous dusty AGN (Hines et al. 1995). It has somewhat cooler IRAS colours than IRAS P09104+4109 (but still warmer than the majority of ULIGs), suggesting its dust is at a lower temperature than that of IRAS P09104+4109. This object also differs from IRAS P09104+4109 in that it does not exist in an X-ray cluster. In fact, this object has yet to be detected in X-rays (Fabian et al. 1996, Ogasaka et al. 1997). It is presumably not associated with a substantial cooling flow. Unlike IRAS P09104+4109, there is no *a priori* reason to expect cold gas in this galaxy.

At high redshifts ($z > 2$), objects which contain dusty AGNs are certainly known, such as IRAS F10214+4724 (Rowan-Robinson et al. 1991) and APM 08279+5255 (Irwin et al. 1998). However the discovery of both of these objects has been serindipitous, often helped by strong gravitational lensing (see Eisenhardt et al. 1996 and Lacy, Rawlings & Serjeant 1998 for IRAS F10214+4724 and Egami et al. 2000 and references therein for APM 08279+5255). More systematic searches are required if we are to address the issues highlighted in the opening paragraph of this section. Surveys done at X-ray wavelengths offer one approach, and have begun to uncover some hot dusty objects (Wilman, Fabian & Gandhi 2000). But these will not find X-ray-quiet dusty AGNs like IRAS F15307+3252. Submillimetre searches with current or future bolometer arrays offer another method, but these will not find dusty AGNs if *all* the dust is hot; unless there is some cold dust present, sources would then fall below the submillimetre confusion limit (Blain et al. 1998). The presence or absence of cold dust in such objects therefore has important implications for cosmological surveys.

We did not detect this cold gas in either object, despite taking very deep integrations. In Section 2, we descirbe the observations. In Section 3, we present the results, compute SEDs, compare IRAS P09104+4109 and IRAS F15307+3252 to other infrared-luminous AGNs, discuss the physical processes that may be responsible for generating a lack of cold gas in these objects, and outline the consequences for systematic surveys of high-redshift dust-enshrouded AGNs. In Section 4 we summarize. Throughout this work, we assume the following cosmological parameters: $H_0 = 65$ km s^{-1} Mpc^{-1}, $\Omega_{\rm matter} = 0.3$, $\Omega_\Lambda = 0.7$.

2 OBSERVATIONS AND DATA REDUCTION

Both sources were observed with the Submillimetre Common User Bolometer Array (SCUBA; Holland et al. 1999) on the James Clerk Maxwell Telescope (JCMT) on Mauna Kea. This instrument consists of two bolometer arrays simultaneously viewing the same region of the sky through a dichroic beamsplitter, arranged in a hexagonal grid with approximately one telescope-beamwidth separating the detectors. We used standard filters: the "short-wavelength array" corresponded to an effective wavelength of observation of $\lambda_0 = 450$ μm and the "long-wavelength array" to $\lambda_0 = 850$ μm.

All observations were conducted in photometry mode, in which the source is positioned onto the central pixel of each array. The data takes the form of a time-dependent voltage reading from each bolometer while the telescope secondary mirror chops the source in and out of the beam, with a throw of 60 arcsec. In photometry mode, one "integration" is defined as a cycle of 9 on-off chopped-pairs positionally offset by 2 arcsec, for a total of 18 seconds of observation. Primary and secondary flux calibration sources were observerd to convert the bolometer voltages into fluxes. The details of the observations are summarized in Table 1, where we list

Table 1. Summary of SCUBA Observations

Source	Date	Number of integrations	Total time on source	$< \tau_{850\,\mu m} >$	$< \tau_{450\,\mu m} >$	$F_{850\,\mu m}$ mJy	$F_{450\,\mu m}$ mJy
IRAS P09104+4109	20 Jan. 1999*	50	900 s	0.25	1.3	4.24 ± 3.36	−19.4 ± 34.2
	18 Mar 2000**	120	2160 s	0.26	1.4	1.44 ± 3.61	−13.35 ± 41.11
	4 Apr. 2000**	280	5040 s	0.39	2.2	3.87 ± 4.18	−29.29 ± 62.79
IRAS F15307+3252	6 Feb. 2000**	175	3150 s	0.45	2.6	3.21 ± 4.36	4.55 ± 83.24
	4 Apr. 2000**	70	1260 s	0.36	2.0	1.79 ± 4.13	6.98 ± 36.23

* Observations performed by K. Hodapp (University of Hawaii)
** Observations in service mode.

integration times, the local atmospheric optical depth at the time of observation, and the measured fluxes.

The alternative positive-and-negative waveform of the chopping secondary was taken out of the voltage stream. Next, the time-dependent variations of the sky brightness were estimated using the signal variations in the bolometers at the periphery of each array, and then were subtracted from the data streams. Two methods of estimating the sky variations (based on using either the mean or the median of the outer bolometer readings) were employed, which proved mutually consistent to within 15% in all cases. We then subtracted the mean of these two sky brightness estimates from the values at the central (on-source) pixel. In all cases, this sky subtraction reduced the uncertainty on the mean source voltage while the improved value remained consistent with the non-sky-subtracted measurements within the latter's larger uncertainties. For each dataset (observing run/source combination), the mean and the variance of the central pixel voltage over time was then determined.

This entire procedure was first performed on the observations of the secondary flux calibrators to determine the flux conversion factor (FCF), by which the mean voltage (in mV) is converted into the observed source flux (in mJy). The following sources were used as flux calibrators: Mars, CRL618, IRAS+16293, OH231.8, and IRC+10216. Their assumed fluxes were taken from the SCUBA calibration web page (http:www.jach.hawaii.edu/JACpublic/JCMT/continuum_observing/SCUBA/). The FCFs were determined independently for each array (i.e. wavelength) and for each observing run. Most of the data were acquired in service mode under "Category 3" weather conditions, which are considered suitable for observations using the Long Wavelength Array but inadequate for use with the Short Wavelength Array. Appropriately, the 850-μm FCFs were measured to be more stable than the 450μm FCFs. During a single observing run, the 850μm FCFs typically varied by $\sim$10 − 15%, and showed run-to-run variations of $\sim$30%. The 450-μm FCFs varied much more widely, up to a factor of two or more, both during a single observing run, and between runs. The variation of the calibrator FCFs was one of the most significant contributions to the (systematic) uncertainty in our results. Faint-object photometry at submillimetre wavelengths is a difficult and error-prone exercise, particularly under below-average weather conditions such as these, and the uncertainty in our final fluxes (see Table 1) is large. Neither IRAS P09104+4109 nor IRAS 15307+3252 were detected within our errors: only upper limits to the source fluxes were obtained.

In addition to these observations, an upper limit to the 350-μm observed-frame (243-μm rest-frame) flux of IRAS P09104+4109 was obtained at the Caltech Submillimeter Observatory in October and December of 1997 using the SHARC camera (Hunter, Benford & Serabyn 1996). Although superior weather conditions were experienced, the collecting area, observing efficiency and stability of the SHARC camera are less than that of SCUBA. This is primarily because the SHARC detector array is one-dimensional and has several inoperative elements near the array center. The upper limit to the flux obtained ($\sim$300 mJy) does not contribute significantly to the 450 and 850 limits discussed here.

3 RESULTS AND DISCUSSION

Combining data from all the runs listed in Table 1, we find the following fluxes: for IRAS P09104+4109, 3.18 ± 2.12 mJy ($3\sigma < 9.54$ mJy) at 850 μm and -18.77 ± 24.25 mJy ($3\sigma < 72.75$ mJy) at 450 μm, and for IRAS F15307+3252, 2.46 ± 3.00 mJy ($3\sigma < 11.46$ mJy) at 850 μm and 6.59 ± 33.22 mJy ($3\sigma < 106.3$ mJy) at 450 μm. For IRAS F15307+3252 the constraints from our results are comparable to those from Yun & Scoville (1998), although at shorter wavelengths. SEDs are plotted in Figures 1 and 2.

3.1 The lack of cold gas in IRAS P09104+4109

It is clear from Figure 1 that IRAS P09104+4109 has very little cold dust; reradiated energy from a cold dust component contributes a fraction below 3.0 % of the bolometric luminosity. The contribution to the 850-μm flux that we would expect from the hot dust responsible for the 25-μm *IRAS* detection accounts for only 1/400 of our observed 2σ upper limit; if this was the *only* dust in the galaxy, it would take several weeks to detect with SCUBA!

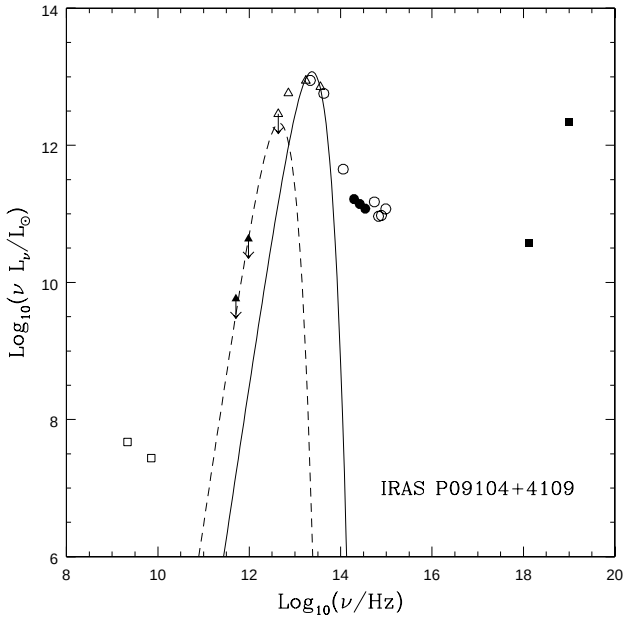

Figure 1. The spectral energy distribuion of IRAS P09104+4109. The points are: open circles – 0.44 μm, 0.55 μm, 0.64 μm, 0.79 μm, 3.8 μm, 10.1 μm and 20 μm (all in the observer frame) from Kleinmann et al. (1988); open squares – radio continuum at 6 cm and 20 cm from Hines & Wills (1993); filled circles – 1.25 μm, 1.65 μm and 2.2 μm from Soifer et al. (1996); open triangles – 12 μm, 25 μm, 60 μm and 100 μm limit from the *IRAS Faint Source Catalog*; filled triangles – 450 μm and 850 μm SCUBA 2σ limits from this work; filled squares – 0.5–7 keV *Chandra* and 14–40 keV *BeppoSax* detections from Iwasawa et al. (2001). The solid line is the best-fitting modified (by a dust emissivity $k \propto \nu^{1.5}$ law) blackbody fit to the *IRAS* detections; this has a dust temperature $T = 206$ K and peaks at 13 μm, but is a statistically poor fit to the three data points. The solid line is the maximum contribution from a cold (37 K) dust component given the limits imposed by our SCUBA data.

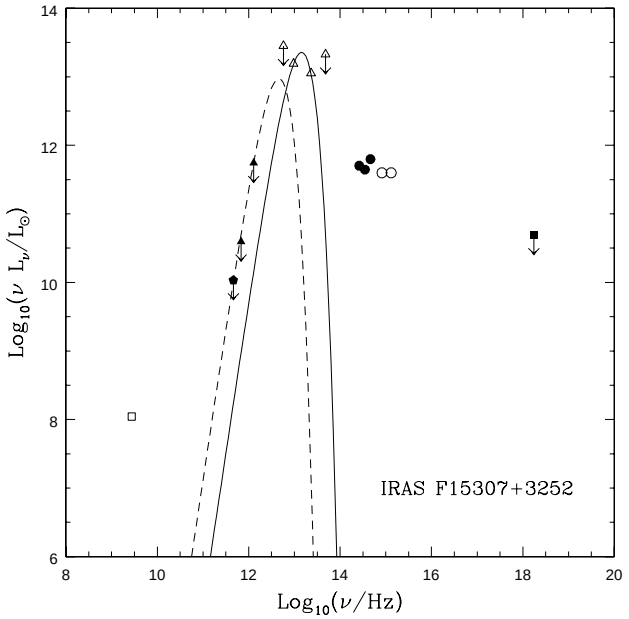

Figure 2. The spectral energy distribuion of IRAS F15307+3252 The points are: open circles – 0.44 μm and 0.70 μm, (all in the observer frame) from Cutri et al. (1994); open square – radio continuum at 21 cm from the FIRST survey of Becker, White & Helfand (1995); filled circles – 1.25 μm, 1.65 μm and 2.2 μm from Soifer et al. (1994); open triangles – 12 μm, 25 μm, 60 μm and 100 μm limit from the *IRAS Faint Source Catalog*; filled triangles – 450 μm and 850 μm SCUBA 2σ limits from this work; filled pentagon – 650 μm lmit from Yun & Scoville (1998); filled squares – 2 –10 keV *ASCA* limit from Ogasaka et al.(1997). The solid line is the best-fitting modified (by a dust emissivity $k \propto \nu^{1.5}$ law) blackbody fit to the *IRAS* detections; this has a dust temperature $T = 126$ K and peaks at 21 μm. The solid line is the maximum contribution from a cold (37 K) dust component given the limits imposed by the data of Yun & Scoville (1998).

The absence of cold dust in a powerful AGN like this is certainly unusual. High-redshift optical quasars often have cold dust (McMahon et al. 1999), so one might expect an infrared quasar like IRAS P09104+4109 to have some too, particularly since the X-ray measurements (Iwasawa et al. 2001) tell us that plenty of cold gas is present.

The solution to this apparent paradox is presumably tied up in the way that gas condenses out of the hot X-ray phase in a cooling flow. If gas condenses in such a way that there is no new star formation, dust generation will be inefficient – carbon atoms associated with this cooling gas are more likely to interact with four hydrogen atoms and become methane rather than with numerous other carbon atoms and become dust grains. This could explain the presence of large amounts of cold X-ray absorbing gas (Iwasawa et al. 2001) and no cold dust. If the cooling flow is also responsible for fuelling the AGN, any star formation that happens along the way must be confined to regions very close to the AGN. Red giants and supernovae associated with this star formation could generate the hot dust seen by *IRAS*.

3.2 The lack of cold gas in IRAS F15307+3252

We also did not detect cold dust in IRAS 15307+3252. In this case the upper limit on the fraction of the bolometric luminosity that could come from a cold dust component is 0.3 %.

While we had no *a priori* reason to expect dust in thie galaxy, this is still a suprising result. High-redshift optical quasars often have cold dust (McMahon et al. 1999). Yet this galaxy, which is opically faint (presumably due to internal extinction) and is such a strong 60-μm emitter, has very little. This result is in some ways more perplexing than the non-detection for IRAS P09104+4109 since the *IRAS* colours are cooler.

These two non-detections have implications for the discovery of hot, dusty AGNs at high-redshift using infrared and submillimetre surveys. We investiate these implications in the rest of this section.

3.3 Application to high redshift

In Figure 3, we plot an optical-infrared vs. infrared-submillimetre colour-colour diagram for the sample of dust-

enshrouded AGNs presented in Table 1. In the rest of this section we will use this diagram to assess the efficacy of finding dusty AGNs at high redshift by a variety of methods. Some particular features worth noting are:

(i) higher temperature sources are to be found near the top of this diagram, but this does not tell us immediately that all sources in this region of the diagram are AGN-powered. For example, IRAS F10214+4724 is to be found near the top of the diagram yet it may derive a substantial fraction of its total luminosity from an obscured starburst (Green & Rowan-Robinson 1996);

(ii) how far to the right of this diagram is a measure of how optically bright an object is, which in turn has implications for our ability to infer the presence of a powerful AGN using optical spectroscopy. For example, the "Q1", "Q2", "CLOV", and "APM" points all represent objects with AGNs so powerful that they likely are responsible for the high bolometric luminosities of the objects;

(iii) this diagram gives no indication of the absolute luminosities of the objects, rather the relative luminosities at different wavelengths. This has implications for the detectability of the objects. For example, APM 08279+5255 is near the top of this diagram yet has been detected at submillimetre wavelengths with SCUBA (Lewis et al. 1998); this is becuase both its bolometric luminosity and gravitational magnification are so high that its submillimetre flux is still measurable. Conversely, IRAS P09104+4109, as we saw here, was not detected, although its spectral energy distribution is perhaps not all that different from that of APM 08279+5255 (note that the increased distance of APM 08279+5255 relative to IRAS P09104+4109 is compensated for by the negative K-correction (see Section 3.3.1);

(iv) Radio and X-ray luminosities can be quite different for objects in similar regions on Fig. 3. This can also have implications regarding the detectability of the different objects.

3.3.1 Submillimetre surveys

The main result of the present paper is that the hot dusty AGNs IRAS P09104+4109 and IRAS F15307+3252 have very little if any cold gas. So if *all* of the dust-enshrouded accretion in the Universe took place at high redshift in objects like these, we would not see them in submillimetre surveys like those carried out with SCUBA (e.g. Smail, Ivison & Blain 1997, Hughes et al. 1998, Cowie & Barger 2000). The only ones we would see in such surveys are (1) extremely luminous, possibly highly-magnified, objects like APM 08279+5255, and (2) the most distant objects at very high redshifts $z > 6$: for sources with dust emissivity $k_\nu \sim \nu^{1.5}$ (e.g. Blain et al. 1999), the observed flux $\sim (1+z)^{4.5} d_L(z)^{-2}$ where $d_L(z)$ is the luminosity distance, so that the negative K-correction more than compensates for the dimming due to the increased distance by a significant amount (see Fig. 4). However, we do not expect the vast majority of sources to fall into either of these two categories.

3.3.2 Infrared surveys

Mid- and far-infrared surveys, like those to be carried out with the *SIRTF* satellite (http://ipac.caltech.edu/sirtf/) offer a far more productive strategy for finding hot dusty AGNs at high redshift: both IRAS P09104+4109 and IRAS F15307+3252 would be easily detected at redshifts $z < 4$. The absence of submillimetre detections at the positions of bright mid-infrared sources would suggest the presence of hot dusty objects. Establishing that such objects are AGN-powered will be more difficult, particularly if they are optically too faint (as both IRAS P09104+4109 and IRAS F15307+3252 would be at high z) to permit spectroscopy with the largest ground-based telescopes. However, the analogy with the lower-redshift objects studied here in the context of the observations and models outlined in Section 1 would be suggestive.

3.3.3 Optical, radio and X-ray surveys

Surveys at other wavelengths can also uncover hot dusty AGNs, but in each case the bias introduced by the selection technique is severe and complete samples cannot be obtained. The reason for this is that so little of the bolometric luminosity of hot, dusty sources emerges outside the far- and mid-infrared wavebands.

Optical surveys can uncover extreme objects like APM 08279+5255 (Irwin et al. 1998). But these represent the rare instances where the AGN is visible directly at rest-frame ultraviolet wavelenghts, possibly because it has burnt through its dust shroud. There still must be enough dust present, however, to allow it to be red enough to be identified in these surveys. It must also be extremely luminous, and in the case of APM 08279+5255, highly magnified. The majority of dusty AGNs at high redshift may well have properties very substantially different from this and would consequently be missed in optical surveys. Both IRAS P09104+4109 and IRAS F15307+3252 would be missed in optical surveys, for example; their optical colours and magnitudes are unremarkable.

Radio surveys can also reveal some dusty AGNs like 3C 318 (Willott, Rawlings & Jarvis 2000). But, as for optical AGNs (Goldschmidt et al. 1999), it seems likely that the majority of such objects are not radio-loud.

Addtionally X-ray surveys would certainly uncover some hot, dusty AGNs like IRAS P09104+4109 (although not IRAS F15307+3252). The presence of a population of sources seen by *Chandra* but not SCUBA (Fabian et al. 2000; see also the discussion of energy budgets and the relation to the local MDO density of Trentham & Blain 2001 and the more recent observations of Bautz et al. 2000, Hornschemeier et al. 2000, and Barger et al. 2001) may have revealed such a population already. Infrared observations of these sources with *SIRTF* will tell us whether or not these objects contain substantial amounts of hot dust. If so, the analogy with the local objects IRAS P09104+4109 and IRAS F15307+3252 outlined in Section 3.2.2 would suggest that they might be AGN-powered. Two X-ray sources have already had *ISO* mid-infrared counterparts identified (Wilman et al. 2000), but longer wavelengths are required to establish the dust temperatures.

4 CONCLUSION

In summary, we have not detected cold, dusty gas in either IRAS P09104+4109 or IRAS F15307+3252. Dust with

Table 2. Objects plotted in Figure 3

Notation	Object + Description (additional to text)	Redshift(s)	Data references
P09	IRAS P09104+4109	0.44	Kleinmann et al. 1988, *IRAS* Faint Source Catalog, this work
F15	IRAS F15307+3252	0.93	Cutri et al. 1994, *IRAS* FSC, this work, Scoville 1997
F10	IRAS F10214+4724	2.29	Rowan-Robinson et al. 1993
APM	APM 08279+5255	3.87	Irwin et al. 1998, Lewis et al. 1998, Ibata et al. 1999
CLOV	H1413+117 "Cloverleaf Quasar"	2.56	Barvainis et al. 1995, Hughes et al. 1997
Q1	Low-z + high L PG quasars $L_{bol} > 10^{12}$ $L_{\odot}$	$0-2$ (mostly < 0.5)	Sanders et al. (1989)
Q2	Low-z + low L PG quasars $L_{bol} < 10^{12}$ $L_{\odot}$	$0-2$ (mostly < 0.5)	Sanders et al. (1989)
Q3	High-z quasars	$3.9-4.7$	McMahon et al. (1999)
Q4	SMM J04135+1027* Submillimetre-selected quasar	2.83	Knudsen et al. (2000)
S1	SMM J02399−0136	2.80	Ivison et al. 1998
S2	SMM J14011+0252	2.56	Ivison et al. 2000
S3	SMM J02399−0134	1.06	Soucail et al. 1999, Smail et al. 2000
HR10	ERO J164502+4626.4 (Object 10 in Hu & Ridgway 1994)	1.44	Dey et al. 1999
3C	3C318	1.57	Willott et al. 2000
4C	4C41.17	3.80	Graham et al. 1994, Archibald et al. 2000
8C	8C1435+63	4.25	Lacy et al. 1994, Archibald et al. 2000
CF1	A2390 cD cooling flow cluster	0.23	Edge et al. 1999
CF2	A1835 cD cooling flow cluster	0.25	Edge et al. 1999
WFG	CXOUJ215333.2+174209 (Object B in WFG00)	0.575	Wilman et al. 2000 (WFG00), Lémonon et al. 1998
S88a	Ultraluminous infrared galaxies	< 0.1	Sanders et al. 1988a
S88b	Warm ultraluminous galaxies	< 0.2	Sanders et al. 1988b

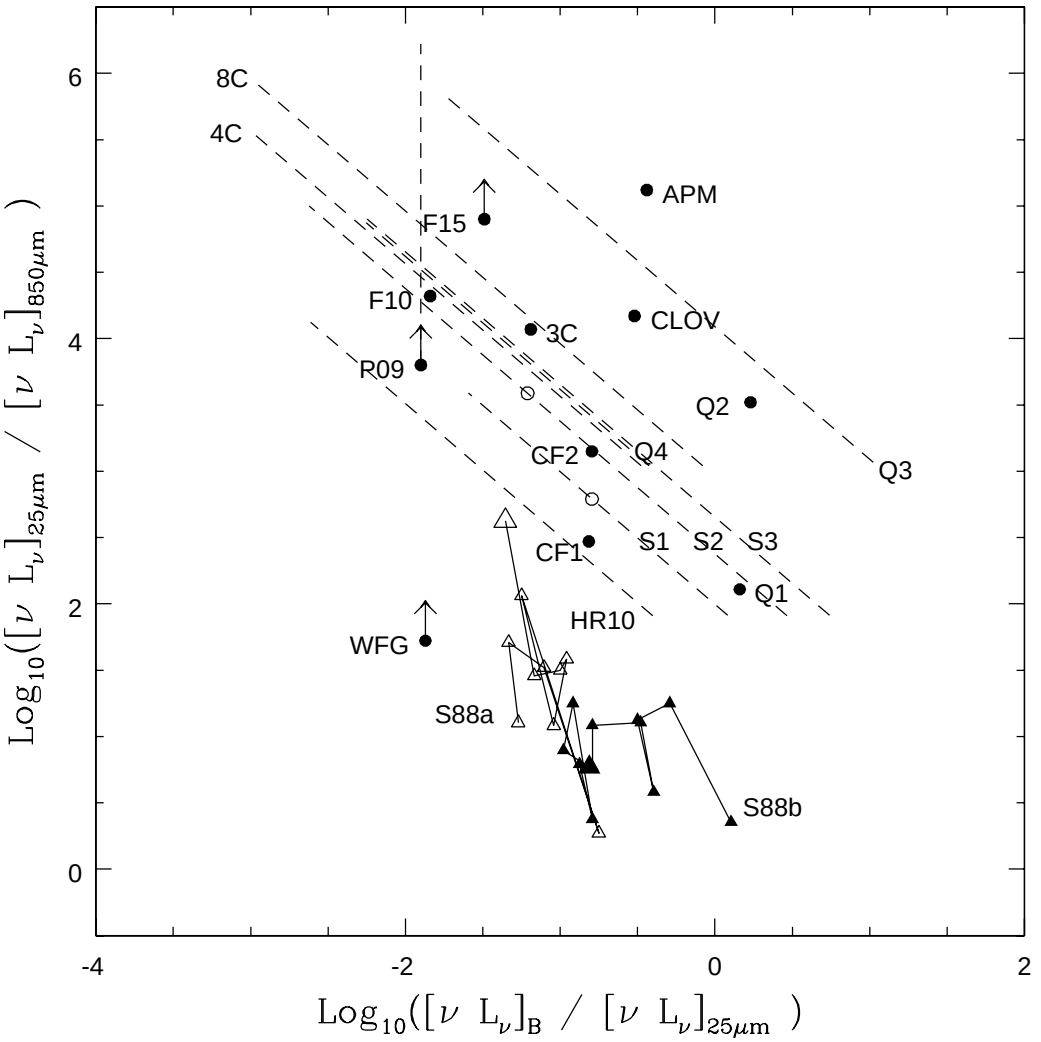

Figure 3. Optical (B) – infrared (25 μm) vs. infrared (25 μm) – submillimetre (850 μm) colour-colour diagram for the objects listed in Table 1. All quantities refer to the rest-frame. The 850-μm luminosities are computed assuming a modified Rayleigh-Jeans spectrum with dust emissivity $k \sim \nu^{1.5}$ (e.g. Blain et al. (1999)). The 25-μm luminosities are computed from *IRAS* measurements, using logarithmic interpolation and/or extrapolation (but never beyond 130 μm) if necessary. The B-band luminosities are computed from K-corrected optical and near-infrared fluxes. The symbols and labels refer to the objects listed in Table 2. Additional comments are: "P09" – The dotted line represents the permitted values given a lower limit to the 850 μm flux equal to the contribution from the hot blackbody that is inferred from the *IRAS* 60 μm and 25 μm detections – the solid line in Fig. 1; "Q3", "Q4", "S1", "S2", "S3", "HR10", "4C" and "8C" – The dotted line represents the locus of permitted values given the absence of a mid-infrared rest-frame detection. The upper-limit to the 25$-\mu$m luminosity comes from IRAS measurements, the lower limit from an extrapolation of the submillimetre SED to mid-infrared wavelengths assuming a modified Rayleigh-Jeans spectrum as above with dust temperatures of 40 K for submillimetre galaxies (Blain et al. 1999; Trentham et al. 1999) and 50 K for quasars (McMahon et al. 1999), and the open circle (where present) is derived from an *ISO* 15-μm detection, converted to a rest-frame 25$-\mu$m flux assuming a power-law spectrum with index $\alpha = -1.7$ (Blain et al. 2000); "WFG" – the mid-infrared luminosity is similarly derived from the *IRAS* 15-μm detection, and the assumed redshift is that derived by Wilman et al. (2000) using the HYPERZ population synthesis code (Bolzonello, Pelló & Miralles 2000). For "Q1", "Q2" and "Q3", median values are plotted. For the "S88a" and "S88b" sequences, each point (the open or filled triangles) represents a galaxy, ordered as in those papers (the large point represents the first galaxy i.e. Arp 220 for "S88a" and IRAS 12071$-$0444 for "S88b") and connected by the lines. For IRAS F10214+4724, APM 08279+5255 and the Cloverleaf quasar, the positions on this diagram have not been corrected for differential magnification (these are strongly lensed sources) and corrections will shift the points downwards and to the left if the sizes of the emitting regions increase with longer wavelength. For the weakly lensed soures (the three SCUBA galaxies), differential magnification (Blain 1999) is a small effect.

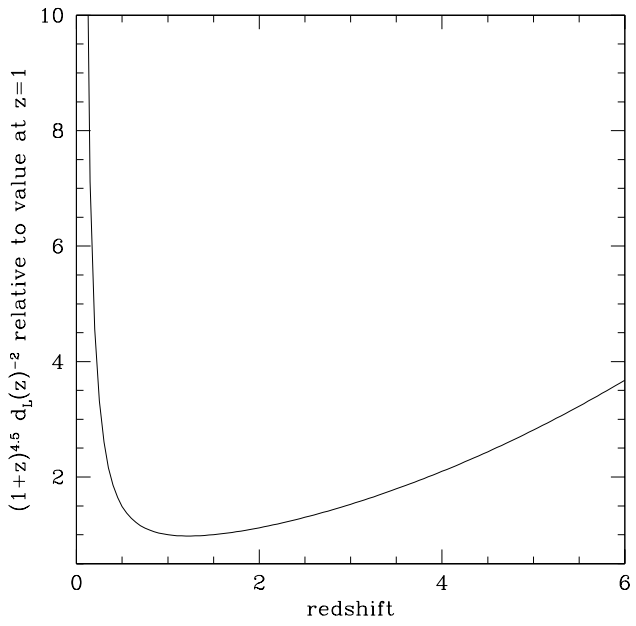

Figure 4. The quantity $(1+z)^{4.5} d_L(z)^{-2}$ as a function of redshift z.

a temperature of 40 K, which is what dominates the bolometric luminosity in most local ULIGs and in the high-redshift SCUBA sources recently discovered in various surveys (e.g. Blain et al. 1999) contributes at most 3 % of the bolometric luminosity of these objects.

These results were somewhat surprising given that IRAS P09104+4109 is associated with a massive cooling flow in which there is independent evidence for cold gas (Iwasawa et al. 2001). Furthermore, cold dusty gas has been detected in a number of optically bright quasars (McMahon et al. 1999) so it was unexpected that it would not be detected in these two objects which are optically faint, presumably due to internal extinction. Some mass of cold dust may still be present, and may be responsible for some of this internal extinction, but it contributes negligibly to the bolometric luminosity.

These two hot dusty galaxies are thought to derive most of their bolometric luminosity from AGNs as opposed to starbursts, based on a number of detailed observational results and models. Dust-enshrouded AGNs that are not seen in optical surveys are thought to be responsible for much of the mass accretion in the Universe that produces the high local density of supermassive black holes seen in the centres of nearby galaxies. Our results suggest that the best way to find such obejcts is to look for powerful mid- and far-infrared emitters in *SIRTF* surveys that have very low submillimtre SCUBA fluxes. Some such objects may have already been seen in joint *Chandra*-SCUBA surveys, but there could also exist a population of hot dusty AGNs (like IRAS F15307+3252) that are not X-ray-loud.

Acknowledgments

We would like to thank Klaus Hodapp for obtaining the 1999 data, and Nick Tothill for assistance with SURF and calibration issues. We also thank Andrew Blain, Aaron Evans, Kazushi Iwasawa and the Cambridge X-ray group for many helpful discussions. This research has made use of the NASA/IPAC Extragalactic Database (NED) which is operated by the Jet Propulsion Laboratory, Caltech, under agreement with the National Aeronautics and Space Association.

REFERENCES

Archibald E. N., Dunlop J. S., Hughes D. H., Rawlings S., Eales S. A., Ivison R. J., 2000, MNRAS, in press (astro-ph/0002083)
Barger A. J., Cowie L. L., Mushotzky R. F., Richards E. A., 2001, AJ, 121, 662
Barvainis R., Antonucci R., Hurt T., Coleman P., Reuter H.-P., 1995, ApJ, 451, L9
Bautz M. W., Malm M. R., Baganoff F. K., Ricker G. R., Canizares C. R., Brandt W. N., Hornschemeier A. E., Garmire G. P., 2000, ApJ, 543, L119
Becker R. H., White R. L., Helfand D. J., 1995, ApJ, 450, 559
Blain A. W., 1999, MNRAS, 304, 669
Blain A. W., 2000, in Lowenthal J., Hughes D., eds, Deep Millimeter Surveys: Implications for Galaxy Formation and Evolution. World Scientific, Singapore, in press (astro-ph/0009012)
Blain A. W., Ivison R. J., Smail I., Kneib J.-P., 1998, in Wide Field Surveys in Cosmology, 14th IAP Meeting. Editions Frontières, Paris, p. 364
Blain A. W., Smail I., Ivison R. J., Kneib J.-P., 1999b, MNRAS, 302, 632
Bolzonella M., Miralles J.-M., Pelló R., Miralles J.-M., 2000, A&A, 363, 476
Bridges T. J., Irwin J. A., 1998, MNRAS, 200, 967
Cardiel N., Gorgas J., Aragón-Salamanca A., 1998, MNRAS, 298, 977
Clements D. L., Sutherland W. J., McMahon R. G., Saunders W., 1996, MNRAS, 279, 477
Cowie L. L., Barger A. J., 2000, Philosophical Transactions of the Royal Society of London, 358, 2133
Crawford C. S., Allen S. W., Ebeling H., Fabian A. C., Edge A. C., 1999, MNRAS, 306, 857
Crawford C. S., Vanderriest C., 1996, MNRAS, 283, 1003
Cutri R. M., Huchra J. P., Low F. J., Brown R. L., Vanden Bout P. A., 1994, ApJ, 424, L65
Dey A., Graham J. R., Ivison R. J., Smail I., Wright G. S., Liu M. C., 1999, ApJ, 519, 610
Edge A. C., Ivison R. J., Smail I., Blain A. W., Kneib J.-P., 1999, MNRAS, 306, 599
Eisenhardt P. R., Armus L., Hogg D. W., Soifer B. T., Neugebauer G., Werner M. W., 1996, ApJ, 461, 72
Egami E., Neugebauer G., Soifer B. T., Matthews K., Ressler M., Becklin E. E., Murphy T. W., Dale D. A., 2000, ApJ, 535, 561
Evans A. S., Sanders D. B., Cutri R. M., Radford S. J. E., Surace J. A., Solomon P. M., Downes D., Kramer C., 1998, ApJ, 506, 205
Fabian A. C. et al., 2000, MNRAS, 315, L8
Fabian A. C., Crawford C. S., 1995, MNRAS, 274, L63
Fabian A. C., Cutri R. M., Smith H, E., Crawford C. S., Brandt W. N., 1996, MNRAS, 283, L95
Fabian A. C., Iwasawa K., 1999, MNRAS, 303, L34
Franceschini A., Bassani L., Cappi M., Granato G. L., Malaguti G., Palazzi E., Persic M., 2000, A&A, 353, 910
Goldschmidt P., Kukula M. J., Miller L., Dunlop J. S., 1999, ApJ, 511, 612

Graham J. R. et al., 1994, ApJ, 420, L5
Green S. M., Rowan-Robinson M., 1996, MNRAS, 279, 884
Haehnelt M. G., Natarajan P., Rees M. J., 1998, MNRAS, 303, 179
Hines D. C., Schmidt G. D., Smith P. S., Cutri R. M., Low F. J., 1995, ApJ, 450, L1
Hines D. C., Schmidt G. D., Wills B. J., Smith P. S., Sowinski L. G., 1999, ApJ, 512, 145
Hines D. C., Wills B. J., 1993, ApJ, 415, 82
Hornschemeier A. E. et al., 2000, ApJ, 541, 49
Hu E. M., Ridgway S. E., 1994, AJ, 107, 1303
Hughes D. et al., 1998, Nat, 394, 241
Hughes D. H., Dunlop J. S., Rawlings S., 1997, MNRAS, 289, 766
Hunter, T. R., Benford, D. J., Serabyn, E., 1996, PASP, 108, 1042
Ibata R. A., Lewis G. F., Irwin M. J., Leh''ar J., Totten E. J., 1999, AJ, 118, 1922
Irwin M. J., Ibata R. A., Lewis G. F., Totten E. J., 1998, ApJ, 505, 529
Ivison R., Smail I., Le Borgne J.-F., Blain A. W., Kneib J. -P., Bezecourt J., Kerr T. H., Davies J. K., 1998, MNRAS, 298, 583
Ivison R., Smail I., Barger A. J., Kneib J. -P.,, Blain A. W., Owen F. N., Kerr T. H., Cowie L. L., 2000, MNRAS, 315, 209
Iwasawa K., Fabian A. C., Ettori S., 2001, MNRAS, 321, L15
Kleinmann S. G., Hamilton D., Keel W. C., Wynn-Williams C. G., Eales S. A., Becklin E. E., Kuntz K. D., 1988, ApJ, 328, 16
Knudsen K. K., van der Werf P. P., Jaffe W., 2000, in Lowenthal J., Hughes D., eds, Deep Millimeter Surveys: Implications for Galaxy Formation and Evolution. World Scientific, Singapore, in press (astro-ph/0009024)
Lacy M. et al., 1994, MNRAS, 271, 504
Lacy M., Rawlings S., Serjeant S., 1998, MNRAS, 299, 1220
Lémonon L., Pierre M., Cesarsky C. J., Elbaz D., Pelló R., Soucail G., Vigroux L., 1998, A&A, 334, L21
Lewis G. F., Chapman S. C., Ibata R. A., Irwin M. J., Totten E. J., 1988, ApJ, 505, L1
McMahon R. G., Priddey R. S., Omont A., Snellen I., Withington S., 1999, MNRAS, 309, L1
Magorrian J. et al., 1998, AJ, 115, 2285
Murphy T. W., Armus L., Matthews K., Soifer B. T., Mazzarella J. M., 1996 AJ, 111, 1025
Ogasaka Y., Inoue H., Brandt W. N., Fabian A. C., Kii T., Nakagawa T., Fujimoto R., Orani C., 1997, PASJ, 49, 179
Rowan-Robinson M., Crawford J., 1989, MNRAS, 238, 523
Rowan-Robinson M., Efstathiou A., 1993, MNRAS, 263, 675
Rowan-Robinson M., 2000, MNRAS, 316, 885
Rowan-Robinson M. et al., 1991, Nat, 351, 719
Rowan-Robinson M. et al., 1993, MNRAS, 261, 513
Salucci P., Szuszkiewicz E., Monaco P., Danese L., 1999, MNRAS, 307, 67
Sanders D. B, Mirabel I. F., 1996, ARA&A, 34, 749
Sanders D. B., Soifer B. T., Elias J. H., Madore B. F., Matthews K., Neugebauer G., Scoville N. Z., 1988a, ApJ, 325, 74
Sanders D. B., Soifer B. T., Elias J. H., Neugebauer G., Matthews K., 1988b, ApJ, 328, L35
Sanders D. B., Phinney E. S., Neugebauer G., Soifer B. T., Matthews K., 1989, ApJ, 347, 29
Smail I., Ivison R. J., Blain A. W., 1997, ApJ, 490, L5
Smail I., Ivison R. J., Owen F. N., Blain A. W., Kneib J. -P., 2000, ApJ, 528, 612
Soifer B. T., Neugebauer G., Armus L., Shupe D. L., 1996, AJ, 111, 649
Soifer B. T., Neugebauer G., Matthews K., Armus L., 1994, ApJ, 433, L69
Soucail G., Kneib J,-P., Bézecourt J., Metcalfe L., Altieri B., Le Borgne J. F., 1999, A&A, 343, L70
Taniguchi Y., Sato Y., Kawara K., Murayama T., Mouri H., 1997, A&A, 313, L1
Trentham N., Blain A. W., 2001, MNRAS, in press (astro-ph/0010186)
Trentham N., Blain A. W., Goldader J., 1999, MNRAS, 305, 61
Willott C. J., Rawlings S., Jarvis M. J., 2000, MNRAS, 313, 237
Wilman R. J., Fabian A. C., Gandhi P., 2000, MNRAS, 318, L11
Yun M. S., Scoville N. Z., 1998, ApJ, 507, 774